Image-potential states on Ni(111): A two-photon-photoemission study

S. Schuppler, N. Fischer, and W. Steinmann
Sektion Physik der Universität München, Schellingstrasse 4, D-8000 München 40, Federal Republic of Germany

R. Schneider and E. Bertel
Abteilung Oberflächenphysik, Max-Planck-Institut für Plasmaphysik, EURATOM-Assoziation, D-8046 Garching, Federal Republic of Germany

(Received 6 February 1990)

The binding energies of the first three members of the image-state Rydberg series on Ni(111) were determined by two-photon photoemission to be -0.80, -0.25, and -0.10 eV, respectively. The effective mass of the $n=1$ image state was measured as $m^*/m=1.12$. We demonstrate that the photon energy for resonant excitation from the occupied $n=0$ surface state to the $n=1$ image state is $k_{\parallel}$ dependent, and from this we obtain an independent confirmation of the $n=0$ state dispersion measured previously by photoemission spectroscopy. The experimental data are well reproduced by a model calculation based on the phase-accumulation model for surface states.

I. INTRODUCTION

A. Spectroscopy of unoccupied states

The spectroscopy of unoccupied states has made considerable progress in recent years. The increasing availability of synchrotron radiation prompted a growing number of studies using photoemission spectroscopy to explore the unoccupied band structure of various surfaces.[1,2] Secondary electron spectroscopy[2,3] provided an independent method for obtaining related information. Both techniques, however, are limited to empty states above the vacuum level. The energy range between the Fermi and the vacuum level became accessible only recently by two different techniques, i.e., inverse photoemission[4] (IPE) and two-photon-photoemission spectroscopy[5] (2PPES). IPE is suitable for probing states both above and below the vacuum level with good **k** resolution but with an energy resolution that is currently limited to about 350 meV.[6]

An alternative technique for exploring states above the Fermi level is two-photon photoemission. In this method intense light from a pulsed laser is used to excite electrons from occupied states below E_F to unoccupied states above E_F. If both the light intensity and the lifetime of the excited particles are large enough a second photon may be absorbed and cause photoemission from the excited intermediate state into free-electron final states propagating into the vacuum. Just as in ordinary photoemission the kinetic-energy distribution of the photoelectrons is measured, and the initial-state as well as the intermediate-state energy can be calculated if the photon energy is known. In this way a superior energy resolution (around 50 meV) combined with an even better **k** resolution than in IPE can be achieved.[7]

Two aspects of the 2PPE technique deserve to be mentioned explicitly. First, the range of usable photon energies is restricted by the sample work function Φ since for higher photon energies strong single-step photoemission causes severe space-charge problems which may be prohibitive for quantitative 2PPE measurements. Second, the cross section for the two-step-photoemission process is directly proportional to the lifetime of the intermediate state. So 2PPE is especially well suited to probe long-lived states and—due to the good energy resolution—their intrinsic linewidths.[8]

B. Image states

The discussion above makes clear that 2PPES is an outstanding tool for the investigation of image states.[5] These states have their origin in the attractive image potential experienced by a charged particle in front of a surface and the reflective properties of the surface itself if they hinder the particle from penetrating into the bulk. As the long-range part of the surface potential is purely electrostatic in nature and decays as $1/4z$ into the vacuum, the image-potential states are expected to form a hydrogenic series converging to the vacuum level.[4]

Electrons trapped in the image potential are confined at the outside of the surface and interact only weakly with the bulk. Therefore they have a long lifetime with an estimated lifetime broadening of less than 50 meV.[9] Accordingly the high resolution obtainable in 2PPES allows a separate analysis of several members of the image-state Rydberg series.

The measurement of the binding energies of the first members in the Rydberg series provides not only the possibility of reconstructing the long-range part of the surface potential, i.e., the classical image potential, but also the validity of common assumptions in the multiple-scattering or phase-accumulation model of surface states[4,9] can be tested rigorously.

C. The multiple-scattering or phase-accumulation model of surface states

This model is a quantification of the simple picture for surface states outlined above. The electron trapped in

front of a surface is considered to form a standing wave in the potential well between the vacuum barrier and the crystal surface. The phase shift Φ_C imposed in the scattering process on the crystal surface is calculated in the simple model from a nearly free-electron (NFE) two-band approximation,[10] and the reflectivity r_C is assumed to be unity. The phase shift Φ_B occurring on the vacuum barrier depends on the detailed model for the surface potential[11–13] and is usually calculated by numerical integration of the Schrödinger equation along the z axis. The reflection coefficient r_B at the vacuum barrier is unity for particles which do not have sufficient perpendicular momentum to surmount the barrier. The condition for surface states in this model then simplifies to $\Phi_C+\Phi_B=2n\pi$ for the round-trip phase shift.

A more realistic model required for the d-band metals, especially for Ni, where the d bands form the lower gap edge, has to abandon the NFE two-band approximation. In addition, the energy dependence of the reflection coefficient r_C should be taken into consideration. A further modification arises if an imaginary part of the bulk effective potential is introduced in order to account for inelastic scattering processes. In Sec. III below we briefly describe such a model calculation which we used to reconstruct the surface potential of Ni(111) from the present experimental data.

II. EXPERIMENT

The present experiments have been carried out on a Ni(111) surface. Full experimental details can be found in Ref. 5 and references therein. A tunable three-stage dye laser is used as the light source for the 2PPE experiment. It is pumped by a XeCl excimer laser with a repetition rate of up to 100 Hz. The dye laser light is frequency doubled in a β-BaB_2O_4 crystal which extends the usable photon energy range to 5.6 eV. p polarization was used and the light was focused onto the sample surface in the UHV chamber. The light intensity had to be restricted to <2 mJ/cm^2 in order to avoid space-charge effects. A simple imaging optics projects the laser spot on the sample onto a screen outside the UHV chamber. The photoelectrons are analyzed in a sectoral hemispherical analyzer with $\pm 2°$ angular resolution and a constant energy resolution set to 150 meV for the present experiments. Dispersion measurements were performed by rotating the sample in front of the analyzer.

The UHV chamber in addition features a gas discharge lamp which allows the recording of one-photon photoemission spectra using the same analyzer. The Ni(111) surface was cleaned in the usual way by argon sputtering and heating cycles, and the cleaning process was monitored by Auger electron spectroscopy. A low-energy electron diffraction (LEED) unit was used to check the sample orientation and the quality of the surface structure.

III. THEORY

Following the original idea of Echenique and Pendry[9] the exact resonance condition defining the existence of surface states can be simplified at $\bar{\Gamma}$ and energies below E_{vac} to minimizing the expression $(1-r_C r_B \exp[i(\Phi_C+\Phi_B)])$ as discussed by Borstel and Thörner.[14] Here r_C and r_B are the crystal and vacuum barrier reflection coefficients, and Φ_C and Φ_B are the corresponding phase shifts. Instead of using the NFE two-band approximation to obtain Φ_C we adopted a Green's-function formalism used for LEED calculations in order to describe the scattering at the crystal potential.[15] The crystal potential was modeled in the muffin-tin approximation with the parameters given for Ni by Moruzzi *et al.*[16] (muffin-tin zero $U_0=-14.46$ eV). A finite imaginary part accounts for inelastic events.[17] The scattering calculation yields both r_C and Φ_C as a function of energy.

The vacuum barrier was constructed following the ideas of Rundgren and Malmström[13] by joining the image potential smoothly to the crystal potential via a third-order polynomial. With the exchange part in the image potential set to zero and the four coefficients in the polynomial being determined by the requirement of smooth continuity this choice leaves three parameters for the fitting procedure: the position of the image plane z_0 and the end points of the polynomial region, z_C and z_B. The origin $z=0$ is placed into the topmost plane of atoms. The barrier phase Φ_B was then calculated as usual by numerical integration of the Schrödinger equation along the z axis.[13]

The three parameters z_0, z_C, and z_B are determined in an iterative procedure. Assuming starting values $z_C=0$ and $z_B=1.5$ Å we varied z_0 to get the correct value for the $n=1$ image state. The position of the $n=0$ surface state is then tuned by shifting z_C. Finally, z_B is used to further minimize the deviations between theoretical and experimental values. Then the next iteration is started by adjusting z_0 and so on until no further improvement can be achieved.

The "theoretical" effective mass was not determined by repeating the full calculation for $k_\parallel \neq 0$. Instead, we use the fact that above the upper gap edge the crystal phase Φ_C is constant, and the image states exhibit a free-electron-like dispersion.[18] Using the Φ_C^{LEED} calculated in the present paper for the upper gap edge (see Fig. 5) we determined the intersection point $[k_\parallel, E_B(k_\parallel)]$ of the image-state band with the upper gap edge.[18] From this intersection point and the measured binding energy at $\bar{\Gamma}$ $[k_\parallel=0, E_B(0)]$, we then derive the effective mass of the image state within the gap. The L_1 critical point energy was taken to be 6.2 eV in order to conserve consistency with the data by Moruzzi *et al.*,[16] and the upper gap edge dispersion was calculated using a combined interpolation scheme.[20]

In concluding this section we would like to mention two previous surface-state calculations for Ni(111). Borstel *et al.*[21] used the one-step model of photoemission to calculate the position of the occupied surface resonance which was observed experimentally by Himpsel and Eastman[22] in ultraviolet photoemission spectroscopy (UPS). The surface potential, however, was modeled by a rectangular step barrier. This calculation correctly represented the occupied crystal-induced state but of course could not reproduce the image states.

Recently Smith and co-workers[23] published a compilation of binding energies of surface states on metals. The data were analyzed in the framework of the phase-accumulation model using the NFE two-band approximation and a Jones-Jennings-Jepsen[12] surface-potential barrier. In the case of Ni(111) the $n=0$ surface resonance and the $n=1$ image state[24] were taken into account. The resulting image-plane distance was found to be 1.23 Å in front of the first atomic layer. The present experiment supplies the binding energies of two additional image states, thus providing a considerably augmented input for theoretical reconstruction of the surface barrier.

IV. RESULTS AND DISCUSSION

Figure 1 shows a series of 2PPE spectra recorded at various electron exit angles θ using a photon energy $h\nu=4.69$ eV. The kinetic energy scale is referred to E_{vac}. The work function for the Ni(111) surface was determined from our *in situ* one-photon-photoemission experiment to be $\Phi=5.25$ eV.

At normal emission in 2PPE a large peak is observed at $E_k=3.89$ eV kinetic energy. The energy E_i of the intermediate state is given by $E_i=E_k-h\nu=-0.80$ eV below E_{vac}. The initial-state energy $E_0=E_k-2h\nu=-5.49$ eV corresponds to a binding energy $E_B=-0.24$ eV with respect to E_F.

From its $h\nu$ dependence it follows that the peak in Fig. 1 results from an unoccupied structure. In view of the intermediate-state energy, its position in the projected bulk band gap, and the dispersion of the peak, this state is easily identified as the $n=1$ image-potential state of Ni(111). The binding energy of -0.80 ± 0.03 eV agrees well with a previous determination in our laboratory.[24]

With increasing exit angle θ, i.e., with increasing $k_\parallel$, the peak shows an upward dispersion accompanied by a significant decrease in intensity. In Fig. 2 the dispersion is displayed in an E versus $k_\parallel$ diagram ($n=1$ state). In order to confirm that the measured dispersion is determined by the intermediate-state dispersion only and not by a combination of intermediate- and initial-state dispersions[5] we measured the dispersion at four different photon energies between 4.69 and 5.25 eV and indeed found no difference in effective mass within the error limits.

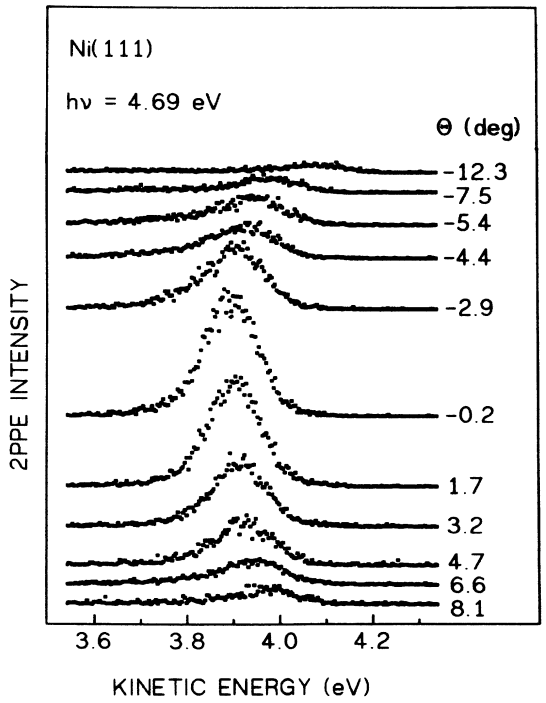

FIG. 1. 2PPE spectra of the $n=1$ image-potential state on Ni(111) at various electron exit angles θ. The spectra are recorded at $h\nu=4.69$ eV photon energy. The kinetic energy is referred to the vacuum level.

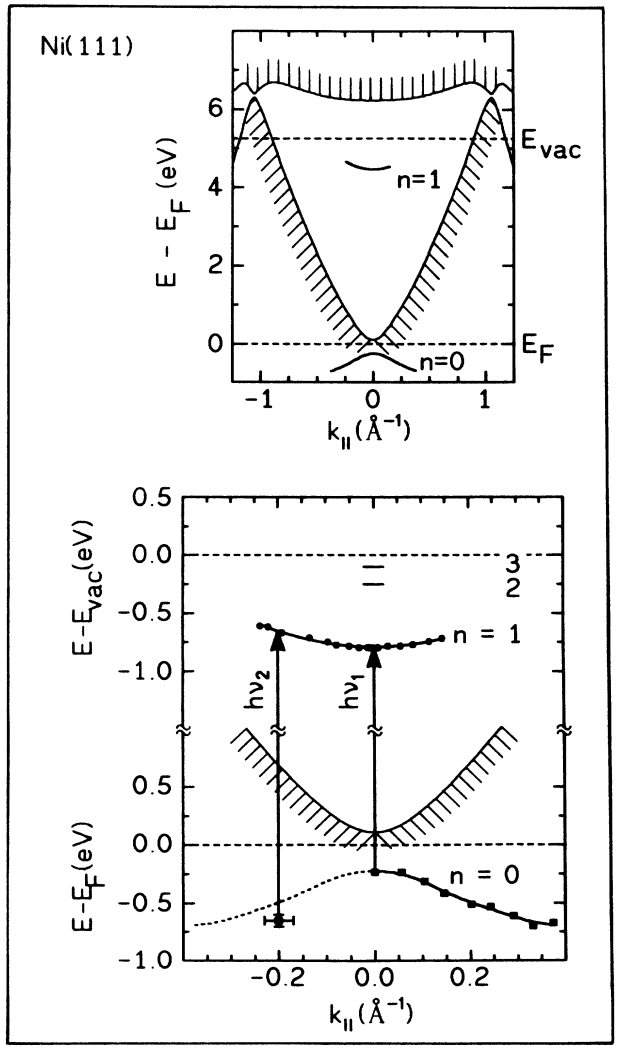

FIG. 2. Upper panel: position of the $n=0$ and $n=1$ surface states in the projected bulk band gap. The band gap was calculated using a combined interpolation scheme (Ref. 20) with data taken from Ref. 19. Lower panel: dispersion $E(k_\parallel)$ of the $n=0$ occupied surface resonance and the $n=1$ image-potential state. The energy of the $n=2$ and 3 image states at $\bar{\Gamma}$ is given as well. The data points on the right-hand side of the $n=0$ state are taken from Ref. 22. The data point on the left is extracted from Fig. 3. The photon energies are $h\nu_1=4.69$ eV and $h\nu_2=5.25$ eV.

The effective mass as derived from the data of Fig. 1 at $h\nu=4.69$ eV and as shown in Fig. 2 is $m^*/m = 1.12\pm0.06$.

This value is at variance with a previous IPE result giving $m^*/m=1.6\pm0.2$.[25] Also the binding energy $E_{B,\mathrm{vac}}=-0.6\pm0.2$ eV obtained in the same IPE measurement is considerably lower but agrees within the large error limits with the present more precise measurement. Recent IPE studies of Ni surfaces indicate that the dispersion measurement in Ref. 25 may have been hampered by residual sample magnetism.[26]

Next we consider the intensity variation of the 2PPE peak shown in Fig. 1. Using UPS, Himpsel and Eastman[22] observed the occupied $n=0$ surface state on Ni(111) at a binding energy $E_B=-0.25$ eV at $k_{\parallel}=0$. This state and its dispersion as measured in the same study are also shown in Fig. 2. In a 2PPE experiment at a photon energy of $h\nu=4.69$ eV a resonant transition from the occupied surface state to the $n=1$ image-potential state is possible at normal emission and results in the high-intensity 2PPE peak at $\theta=0$. With increasing $k_{\parallel}$ the occupied surface state disperses downward, and the image state upward. Therefore at finite exit angles θ the resonance condition is no longer fulfilled with fixed photon energy. The initial states are then bulk Bloch states which have a much smaller overlap with the image state as compared to the occupied surface state. Accordingly the intensity of the 2PPE peak in Fig. 1 drops rapidly with increasing exit angle.

The intensity variation of the 2PPE peak at $h\nu=4.69$ eV as a function of $k_{\parallel}$ is shown in Fig. 3 (solid dots). From Fig. 2 it is obvious that at photon energies larger than $h\nu=4.69$ eV the resonance condition for surface-state to image-state transitions should again be fulfilled at finite $k_{\parallel}$ values. We have tested this assumption in a 2PPE measurement at $h\nu=5.25$ eV and found the intensity variation marked by open squares in Fig. 3. As expected, the resonance in this case occurs at $k_{\parallel}=0.2$ Å^{-1}, which also yields an independent determination of the initial-state dispersion. The corresponding transition is shown as well in Fig. 2.

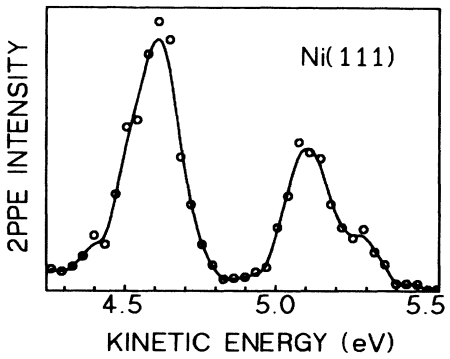

FIG. 4. 2PPE spectrum of the first three image states of Ni(111) recorded at $h\nu=5.25$ eV with an energy resolution of $\Delta E_{\mathrm{FWHM}}=150$ meV.

Exploiting the superior resolution of the 2PPE experiment we also tried to measure the binding energies of the higher ($n\geq2$) members of the image-potential state series. Such a measurement, however, is far from being trivial. On the one hand, the photon energy must be approximately equal to the work function Φ in order to provide sufficient quantum energy for excitations from occupied states to the higher image-potential states. On the other hand, the photoelectron yield increases dramatically as the photon energy approaches Φ due to the onset of one-photon photoemission.[27] As a consequence space-charge effects occur and the measured binding energies become unreliable.[28] We were not able to eliminate these shifts on the absolute energy scale for $h\nu\approx\Phi$. By carefully examining different photon energies, however, we found the energy intervals between the Rydberg-series members to be insensitive to the space-charge effects. Thus the absolute binding energies of $n\geq2$ image-potential states can be determined from their energy distance to the $n=1$ image state and the absolute binding energy of this state. This latter binding energy in turn can be measured at photon energies far below the work

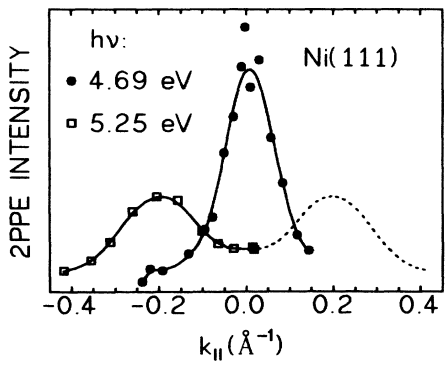

FIG. 3. Intensity of the $n=1$ image-state-related 2PPE signal as a function of $k_{\parallel}$ for two different photon energies. For $h\nu=4.69$ eV a resonance occurs at $k_{\parallel}=0$, whereas for $h\nu=5.25$ eV the resonance is observed at $k_{\parallel}=0.2$ Å^{-1}.

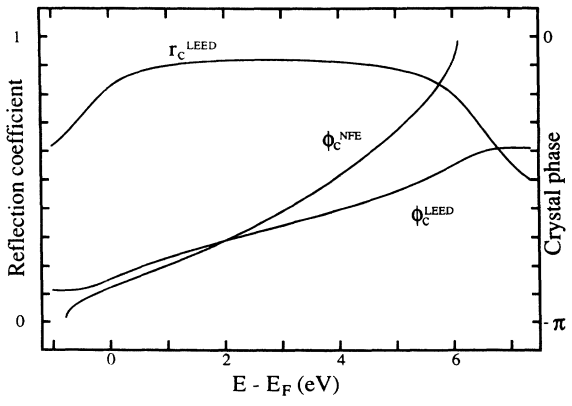

FIG. 5. Comparison between the crystal phase Φ_C^{NFE} obtained from the NFE two-band approximation and Φ_C^{LEED} obtained from a LEED-type multiple-scattering calculation. The crystal reflection coefficient r_C is also shown.

TABLE I. Summary of the experimental and theoretical binding energies for the Ni(111) surface states. Also included are the effective mass for the $n=1$ image state and the parameters used for modeling the surface barrier.

Type of surface state	Shockley state	Image-potential states			
Binding-energy reference	$E-E_F$ (eV)		$E-E_{vac}$ (eV)		Effective mass m^*/m
n	0	1	2	3	for $n=1$
Experiment	-0.25[a]	-0.80 ± 0.03	-0.25 ± 0.05	-0.10 ± 0.05	1.12 ± 0.06
Theory	-0.289	-0.771	-0.211	-0.094	1.08
Surface potential parameters	$U_0=-14.46$ eV,[b] $z_0=1.42$ Å, $z_C=-0.34$ Å, $z_B=2.3$ Å				

[a]Reference 22.
[b]Reference 16.

function where no space-charge effects occur.

Figure 4 shows a 2PPE spectrum measured at $h\nu=5.25$ eV at normal exit $\theta=0$. The largest peak at $E_{kin}=4.6$ eV corresponds to the (slightly space-charge shifted) $n=1$ image-potential state. A second peak appears at 5.1 eV kinetic energy and is assigned to the $n=2$ image state. The $n=3$ image state is not yet completely resolved in Fig. 4 but appears as a shoulder at $E_{kin}=5.3$ eV. From a least-squares analysis of several spectra recorded at slightly different photon energies we arrive at the numbers presented in Table I for the binding energies of the $n=1,2,3$ image-potential states on Ni(111). These data are well reproduced by the results of the present theoretical calculation.

The image-plane distance $z_0=1.42$ Å is considerably larger than the average value $\langle z_0\rangle=1.23$ Å obtained by Smith *et al.*[23] This is mainly a consequence of the different crystal phase Φ_C found in our calculation. Figure 5 shows a comparison between the crystal phase Φ_C^{LEED} as calculated in the present scheme and Φ_C^{NFE} derived from the NFE two-band approximation using an image plane $z_0=1.23$ Å and a crystal potential $U_0=-15.9$ eV. The crystal phase Φ_C^{LEED} does not start exactly from $-\pi$ at the lower gap edge which is mainly an effect of s-d hybridization.[14] Nevertheless, in the lower part of the band gap Φ_C^{LEED} follows closely Φ_C^{NFE}. As the energy approaches E_{vac}, Φ_C^{LEED} deviates rather seriously from Φ_C^{NFE}, which is mainly due to damping. The larger negative value of Φ_C^{LEED} calls for a larger image-plane distance in order to correctly represent the experimental binding energies of the image states. One should be aware, however, that the image-plane distance is conceptually model dependent, and therefore not the absolute values but rather the trends for different surfaces and different metals are of physical significance. It is interesting to note that the Ni(111) surface is indeed special in that it exhibits the largest z_0 value found so far.[23] The present data confirm this notion.

In addition to the crystal phases Fig. 5 also shows the behavior of the reflection coefficient r_C as a function of energy. In the energy range of the image states it is nearly constant and close to unity. At the position of the occupied surface state, however, r_C varies rapidly with energy and therefore influences the $n=0$ surface-state binding energy which is not taken into account by the simple phase-matching procedure. Finally we note that the theoretical binding energies of the image-potential states obtained in the present scheme deviate only slightly from the Rydberg series predicted by the simple hydrogenic model.

V. SUMMARY

We have measured the $n=1$ image-potential state on the Ni(111) surface in a high-precision 2PPE experiment. Its dispersion corresponds to an effective mass $m^*/m=1.12$, which is consistent with the present theoretical concepts but not with the value found by inverse photoemission. In addition, the binding energies of the $n=2$ and image states were determined. The experimental surface-state binding energies can consistently be reproduced in a phase-accumulation model where conventional LEED calculation techniques have been used to obtain the crystal phase shift and reflection coefficient. Measurements on the observed surface states with better energy resolution are in progress in order to determine the lifetime broadening of the image states.

ACKNOWLEDGMENTS

We gratefully acknowledge stimulating discussions with W. Moritz and Th. Fauster. The work was supported by the Deutsche Forschungsgemeinschaft (DFG).

[1]R. Courths and S. Hüfner, Phys. Rep. **112**, 53 (1984).
[2]A. Goldmann, G. Rosina, E. Bertel, and F. P. Netzer, Z. Phys. B **73**, 479 (1989).
[3]R. F. Willis and N. E. Christensen, Phys. Rev. B **18**, 5140 (1978); N. E. Christensen and R. F. Willis, J. Phys. C **12**, 167 (1979).
[4]N. V. Smith, Rep. Prog. Phys. **51**, 1227 (1988).
[5]W. Steinmann, Appl. Phys. A **49**, 365 (1989).

[6]V. Dose, in *Lectures on Surface Science,* edited by R. G. Castro and M. Cardona (Springer, Berlin, 1987), p. 181.
[7]K. Giesen, F. Hage, F. J. Himpsel, H. J. Riess, and W. Steinmann, Phys. Rev. Lett. **55**, 300 (1985).
[8]H. B. Nielsen, G. Broström, and E. Matthias, Z. Phys. B **77**, 91 (1989).
[9]P. M. Echenique and J. B. Pendry, J. Phys. C **11**, 2065 (1978); P. M. Echenique, F. Flores, and F. Sols, Phys. Rev. Lett. **55**, 2348 (1985); P. M. Echenique and J. B. Pendry, J. Phys. C **19**, 5437 (1986); P. de Andres, P. M. Echenique, and F. Flores, Phys. Rev. B **35**, 4529 (1987).
[10]N. V. Smith, Phys. Rev. B **32**, 3549 (1985).
[11]E. G. McRae and M. L. Kane, Surf. Sci. **108**, 435 (1981).
[12]R. O. Jones, P. J. Jennings, and O. Jepsen, Phys. Rev. B **29**, 6474 (1984).
[13]J. Rundgren and G. Malmström, J. Phys. C **10**, 4671 (1977); G. Malmström and J. Rundgren, Comput. Phys. Commun. **19**, 263 (1980).
[14]G. Borstel and G. Thörner, Surf. Sci. Rep. **8**, 1 (1988).
[15]J. F. L. Hopkinson, J. B. Pendry, and D. J. Titterington, Comput. Phys. Commun. **19**, 69 (1980).
[16]V. L. Moruzzi, J. F. Janak, and A. R. Williams, *Calculated Electronic Properties of Metals* (Pergamon, New York, 1978).
[17]A. Goldmann, V. Dose, and G. Borstel, Phys. Rev. B **32**, 1971 (1985).
[18]K. Giesen, F. Hage, F. J. Himpsel, H. J. Riess, W. Steinmann, and N. V. Smith, Phys. Rev. B **35**, 975 (1987).
[19]H. Eckardt and L. Fritsche, J. Phys. F **17**, 925 (1987).
[20]N. V. Smith and L. F. Mattheiss, Phys. Rev. B **9**, 1341 (1974).
[21]G. Borstel, G. Thörner, M. Donath, V. Dose, and A. Goldmann, Solid State Commun. **55**, 469 (1985).
[22]F. J. Himpsel and D. E. Eastman, Phys. Rev. Lett. **41**, 507 (1978).
[23]N. V. Smith, C. T. Chen, and M. Weinert, Phys. Rev. B **40**, 7565 (1989).
[24]K. Giesen, F. Hage, F. J. Himpsel, H. J. Riess, and W. Steinmann, Phys. Rev. B **35**, 971 (1987).
[25]A. Goldman, M. Donath, W. Altmann, and V. Dose, Phys. Rev. B **32**, 837 (1985).
[26]M. Donath and K. U. Starke (private communication).
[27]When increasing the photon energy up to a value close to the sample work function we observed an exponential increase of the photoelectron yield in the 0-eV peak. The slope of the increase could be shown to depend inversely on the sample temperature. This effect can be interpreted as one-photon photoemission from thermally occupied states above the Fermi energy. As the density of states at E_F is large for Ni, a significant contribution of one-photon photoemission may occur even for photon energies several kT below the work function.
[28]G. D. Kubiak, Surf. Sci. **201**, L475 (1988).